Article:
Stephen, J.T., Hardwick, C., Beaty, P. et al. (2 more authors) (2019) Ultrasonic monitoring of insulated block joints. Proceedings of the Institution of Mechanical Engineers. Part F: Journal of Rail and Rapid Transit, 233 (3). pp. 251-261. ISSN 0954-4097

https://doi.org/10.1177/0954409718791396

Ultrasonic Monitoring of Insulated Block Joints

J.T. Stephen[1], C. Hardwick[2], P. Beaty[2], *M.B. Marshall[1] and R. Lewis[1]

[1]Department of Mechanical Engineering, University of Sheffield, Mappin Street, Sheffield S1 3JD, UK.

[2]LB Foster Rail Technologies (UK) Ltd, Stamford St, Sheffield, S9 2TX, UK

*Corresponding author

ABSTRACT

Insulated block joints are essential components used in railway tracks, to separate them into circuits used for train detection and signalling. However, they also represent a week point in the track system, and have a finite life. Condition monitoring of these components in order to plan preventative maintenance is currently labour intensive, and can lead to significant costs for the rail operator.

In this study, IBJ's were fatigued via shear load, whilst being condition monitored for degradation using a normally incident ultrasonic technique. Tests were also initially performed on lap-joints and shear specimens to further understand the response of the ultrasonic signal to failure of the adhesive layer under controlled conditions. Dynamic reflection coefficients as well as applied load were recorded in all tests, and results compared to failure zones on the specimens.

The results showed that the ultrasonic technique was able to determine the on-set of failure and de-bonding of the adhesive layer, as well as degradation and wear. The technique was also able to highlight differences in performance between two different liners, pultruded glass reinforced polyester resin and a flexible glass fibre sheet, with the latter showing improved resistance. The outcomes of this study have highlighted the viability of condition monitoring IBJs using an ultrasonic approach, and have provided a basis for a future field trial.

KEY WORDS

Insulated block joints, cyclic shear load, fishplates, rail, ultrasonic reflection.

1 INTRODUCTION

Insulated block joints (IBJs) are bolted adhesive joints that are used to join sections of railway track together. They are classed as a mechanical connector and are made up of fishplates and fasteners (bolts and nuts) that attach the fishplates to the web of the rail, and have an insulating layer adhesively bonded at the interface. IBJs are typically used every few kilometres along railway tracks to separate them into track circuits used for train detection and signalling, but also introduce weak points causing high maintenance schedules and service disruption that represent a significant industry cost.

Research has been undertaken on the improvement of such joints, and has been focused in the areas of design and materials, support structures and wheel/track interaction [1-4]. Most of the research work has used FE methods to simulate the stresses and strains developed at such joints [5-7], while experimental studies have frequently investigated the fatigue life of joint bars, stress concentrations in the rails and fishplates caused by bolt holes, stresses due to head contact, and head-free joint bars [8-10].

Little research has been undertaken into the condition monitoring of such joints, despite rail joints being a critical component from a safety perspective in a rail network [11, 12]. Peltier and Barkan [13] investigated the effect of longitudinal loads over time using strain-gauge based techniques. They measured changes in the tensile strain in an IBJ, and using additional results from finite element methods, related it to loss of epoxy bonding in the IBJs. However, assumptions were made that the joints response to dynamic vehicle loads, daily variation in environmental temperature and impact factors such as support of the track modulus will not impact the measurements.

In many cases, deterioration of IBJs initiates at the adhered junction between the fishplate and rail web [14], and if appropriate maintenance is not undertaken, will result in the formation of a conductive rail joint of low integrity [13]. At present, such defects are detected via visual means, however these are unable to determine de-bonding of the epoxy at the clamped interface, are labour intensive and prone to human errors [15]. Therefore, timely and reliable information about the condition at the joints interface, with minimal human intervention, will be beneficial in order to undertake preventative maintenance. Information obtained from monitoring could also feedback into optimising IBJ design.

Non-intrusive ultrasonic techniques have been previously used to measure contact pressure in bolted joints and machine parts [16, 17]. Relaxation and loosening in bolted joints has also been measured using ultrasound [18]. Previously, ultrasound has been used to determine de-bond in adhesive structures found in aerospace and automotive industries, and in some cases has been integrated with production processes as a quality control technique [19-21]. Therefore, in this study, a novel ultrasonic technique will be used to characterise and monitor the behaviour of the insulated adhesive interface of an IBJ, as it is fatigued to failure, with an overall aim to develop a condition monitoring approach for these components.

2 CONTACT SURFACE AND ULTRASOUND

In a real engineering interface, a perfect bond does not exist. Instead when surfaces are loaded together they mostly interact at the junctions of the surface roughness/asperities, with air gaps at the void between the asperities [22]. When normal ultrasound waves are incident at an interface, the waves are partially reflected at the interface (Figure 1a). Sound is transmitted at the asperity junctions, and reflected at the metal-air interface due to the trapped air pockets. The quantity of sound transmitted depends on the wavelength of the sound wave relative to the air gap.

The relative amplitude of the ultrasound wave incident at the boundary that is reflected from it is known as the reflection coefficient for a displacement wave amplitude, R, and is described by:

$$R = \frac{z_1 - z_2}{z_1 + z_2} \qquad 1$$

where z is the acoustic impedance and subscripts 1 and 2 refer to acoustic impedance for the material on either side of the boundary. The acoustic impedance is equal to the product of wave speed and density for a given material.

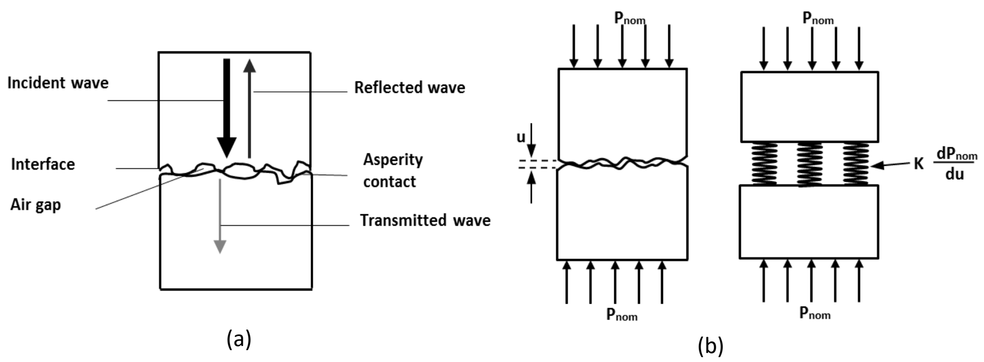

Figure 1: (a) Ultrasonic reflection at a rough surface interface and (b) Schematic representation of an interface using the spring model.

In a study conducted by Kendall and Tabor [23] on rough surface contacts, and followed up by Tattersall [24] on adhesive layers, the asperity interactions of the interface were modelled as a series of parallel springs (Figure

1b). They found that when the wavelength of the ultrasound was large compared to the scale of the surface roughness, the interface behaved as a unique reflector, and that the reflection coefficient depends on the interfacial stiffness, *K*, with the relationship between them governed by:

$$R = \frac{Z_1 - Z_2 + \frac{i\omega Z_1 Z_2}{K}}{Z_1 + Z_2 + \frac{i\omega Z_1 Z_2}{K}} \qquad 2$$

where ω is the angular frequency of the sound wave. The stiffness of the interface is the normal contacting pressure, P_{nom}, required to cause a unitary approach of the mean lines of the two surfaces, and is quantified per unit area. Thus:

$$K = -\frac{dP_{nom}}{du} \qquad 3$$

where *u* is the separation of the mean lines of roughness of the two surfaces. When the surfaces are just touching the interfacial stiffness is zero (i.e. the asperities can deform easily and separation between surfaces can be reduced), and rises to infinity when complete conformance occurs at the interface (i.e. deformation of asperities and reduction of separation between surfaces is no longer possible). Additionally, Drinkwater *et al.* [25] demonstrated that the spring model could be applied to reflection data from rough surface interfaces for ultrasound frequencies up to a maximum of 50 MHz, depending on the materials and surface roughness of the contact under investigation.

3 EXPERIMENTAL PROCEDURE

Figure 2 shows an IBJ used to join two rails together. As highlighted, the IBJ uses both bolted joints as well as an adhesive layer in its construction, with both of these connection mechanisms requiring condition monitoring in the planned experimental study. Stresses in IBJ's are also quite complex, with transverse loading of an IBJ resulting in shear stresses in the glued layer. Similarly, any bending of the loaded system will also lead to an additional stress on this layer. A series of pre-tests were first performed in order to characterise the glued interface of the IBJs, and separate any changes in this interface from relaxation of the bolted joints. The pre-tests comprised of a tensile lap-shear test undertaken on specimens adhered with the IBJ interface glue, and a further shear test performed on a section of IBJ, repeated with two liner types. Following on from these pre-tests, the last stage of the study consisted of shear testing of complete IBJs under full dynamic load conditions.

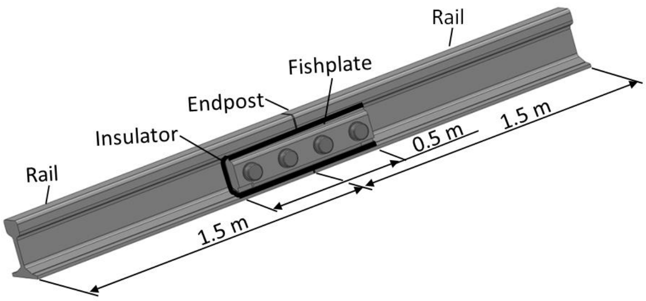

Figure 2: bolted adhesive glued insulated block joint.

3.1 Shear Testing of Insulated Lap Joints and IBJ Sections

Figure 3 shows the test specimens used in the pre-test. The insulated lap-joints (Figure 3a), were produced from two identical steel plates of dimension 100 mm × 25 mm × 1.6 mm, with the insulating material glued between them. Samples were produced with two different liner materials, a pultruded glass reinforced polyester resin and a flexible glass fibre sheet, and were reflective of the IBJ's to be tested subsequently. Manufactured insulated lap joint samples were instrumented, and spacers attached at either end in order to ensure the samples were loaded without twist. Samples were instrumented using Piezoelectric (lead zirconate titanate) ultrasonic transducers with a centre frequency of 10 MHz, a nominal diameter of 7.1 mm and thickness of 0.2 mm, directly bonded to the specimens using M-bond 200 (Vishay) adhesive. Coaxial data wires were then soldered to the terminals of the transducers, and the transducer assembly potted in order to prevent damage. The joints were tested in pure shear on a Tinius Olsen Tensometer under constant displacement control at a rate of 1 mm/min until shear of the glued joints occurred.

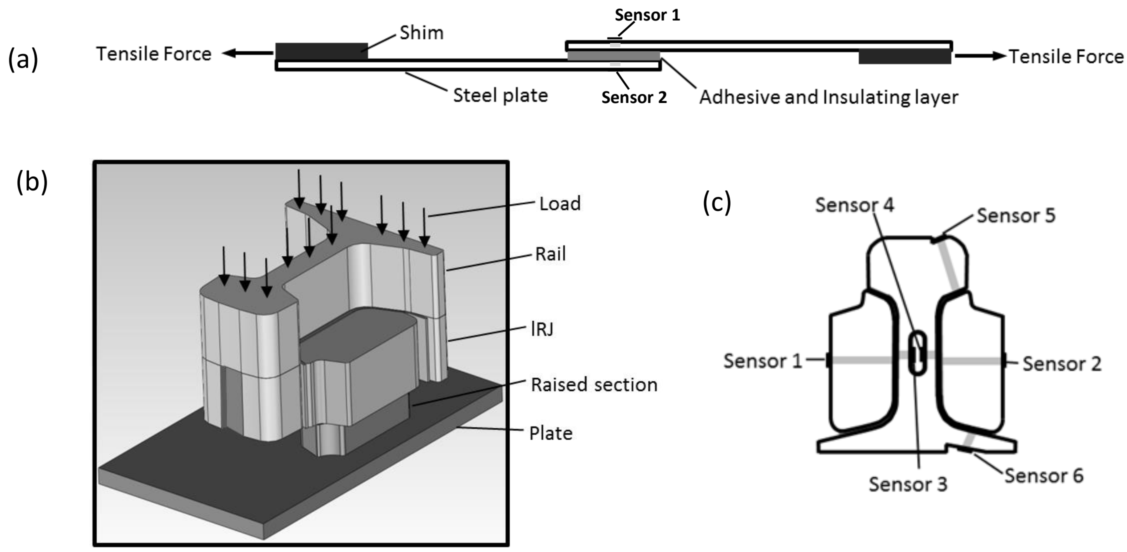

Figure 3: Diagram of the of the test specimens (a) the insulated lap-joint, (b) the IBJ and (c) sensors on the IBJ.

Figure 3 (b) shows the shear test sample and test arrangement. As shown in the Figure, the instrumented IBJ was positioned on a mounting plate with a raised section corresponding to the area of the fishplate. A piece of rail is similarly installed above the test sample, and the specimens aligned. In this way, when load is applied, a shear force is generated in the glued layer of the specimen, between the rail and fishplate components of the IBJ. As in the case of the insulated lap joint samples, two different liners have been tested, with each sample instrumented with 10 MHz ultrasonic transducers. Figure 3 (c) shows the bonded transducers, along with the anticipated paths between the sensors and the interfaces of interest. As shown in the Figure, a series of six transducers have been used, with four focusing on the web / fishplate interfaces, and a further two at the top and bottom. This arrangement has been chosen with the aim of both understanding how the ultrasonic signals respond to shear failure of the glued joint, as well as which part of the joint fails first. Shear testing of the specimens was undertaken on a displacement controlled hydraulic compression rig. Prior to testing, the parallelism of the set-up was checked (the IBJ specimen relative to the load transfer plates) in order to make sure an even load was applied to the specimen. A constant displacement vertical load was then applied to the aligned specimen, and the test was completed once the interface between the two components had sheared.

It should also be noted that in both of the pre-tests detailed, load and displacement were recorded on a common time stamp, with a similarly synchronised ultrasonic measurement performed in order to condition monitor the sample. Ultrasonic signals were generated using a PC based FMS100 System, which contained an ultrasonic pulser-receiver (UPR) and digitiser. This was used to generate and receive ultrasonic reflections from the clamped adhesive interface through the utilised transducers (Figure 4). In all cases, the transducers were excited with a 100 ns duration 25 V ‘top-hat’ signal, and 1 kHz a pulser repetition rate used. Reflected signals from the interface were digitised with *12-bits* resolution at a rate of 100 MHz. The digitised reflected signals were recorded for post processing. Before testing in each case, a reference signal was recorded from each interface. The reference along with the reflected signals obtained during the test, were then used to determine reflection coefficient.

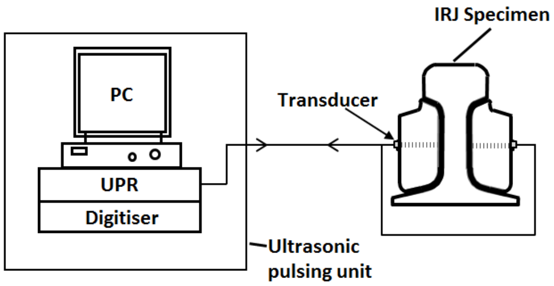

Figure 4: Schematic diagram of the ultrasonic equipment and two of the sensors used on the IBJ Section.

3.2 Full Scale IBJs

IBJ specimens were prepared for test at LB Foster Rail Technologies in Sheffield, United Kingdom. The joints were used to join two sections of standard 3m flat bottom rail (EN13674-56E1) together, and were of the four-bolt, adhesive glued type (Figure 2). Two different specimens were manufactured with different insulating materials, which were pultruded glass reinforced polyester resin (LBFR1) and flexible glass fibre sheet (LBFR2). With the latter case being an improved design, with reduced manufacturing tolerances and an increased stiffness at high load. In each case, the specimens were attached to 1.1/8” swage fasteners resulting in a clamping force of 260 kN, representing a UK standard.

3.2.1 Ultrasonic instrumentation of specimens & test arrangement

The IBJs were instrumented with the previously detailed ultrasonic transducers. Eight piezoelectric transducers were permanently bonded to each of the test specimens with M-bond 200 (Vishay) adhesive, four on each of the two fishplates (Figure 5). The transducers were bonded in the same way as in the pre-test in close proximity to the fasteners (bolt and nut respectively), as a previous study [16] has indicated that when condition monitoring relaxation of bolted joints via the clamped interface pressure distribution, the distance from the bolt hole is a key factor with respect to the accuracy of the technique.

The structure of the IBJs was left as-received, with the surface areas where the transducers were bonded cleaned with a mild abrasive agent and degreased, in order to remove contamination so as to ensure good acoustic coupling.

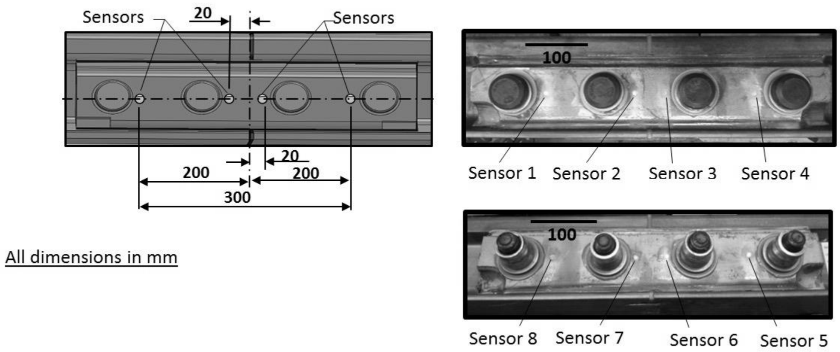

Figure 5: Bonded transducers on the specimen (both sides).

The instrumented IBJs were tested via a 4-point bending arrangement (Figure 6), as this meant maximum deformation occurred at the centre of the joint, with negligible stress-concentrating influence from the loading points [26]. In this sense, a uniform stress field was developed, and additionally a significant joint load could also be developed to test the specimens to failure.

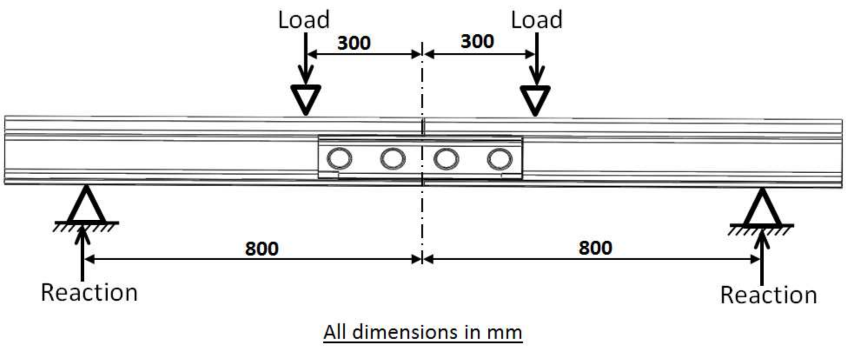

Figure 6: Schematic diagram of the experimental setup of the IBJ.

3.2.2 Test procedure

The previously detailed ultrasonic apparatus was connected to the sensors on the IBJ specimen, with the 4-point load arrangement achieved on a hydraulic fatigue rig (dual actuator, 25 kN maximum rate load, 2Hz frequency). As well as monitoring load during a test, displacement of the joint centre was also recorded using an LVDT (Linear Variable Differential Transducer), with a time stamp used to correlate these two data sets.

Using the detailed test arrangement, a loading programme was developed to investigate both the fatigue of the joints as well as their ultimate failure (Table 1). The first load was chosen to replicate a rail on a soft foundation (low track modulus) with maximum static force as applicable to the UK rail network (25 ton axle load) [27]. This represents in-service conditions. The second load represents that of the most stringent qualification test that could be found in a similar section of rail size [28]. In order to test the operational limit of the component, the highest load represents a 2.5 factor of safety over the first load and is close to the maximum that can be achieved in the test set-up. Finally, the third load was selected to be the average of the second and the highest loads. In this case, the application of the third and the highest loads were selected to accelerate the failure of the joint, in order to condition monitor the component through to failure. During the testing the response from the ultrasonic transducers was monitored using the previously detailed equipment and instrument settings, and both reference and reflected pulses captured for post-processing. Upon completion of the testing of the first IBJ, an identical process was followed for the second joint under test.

Table 1: Loading of the IBJs

Applied load (kN)	Equivalent bending moment (kNm)	Number of cycles (million)
161	40	0 - 0.5
270	67	0.5 – 1.0
337	84	1.0 – 1.5
404	101	1.5 – 2.0

4 RESULTS

The dynamic reflection coefficient was calculated by dividing the reflected signal during a test by the reference signal. As discussed, typically the reference signal is recorded with an air counter face. Therefore, by dividing the reflected signal by the reference value, attenuation is removed, and the reflection coefficient is a numeric descriptor for the degree of contact with respect to the unloaded case. Using the spring model and a calibration procedure, interfacial stiffness and contact pressure can then be calculated respectively. However, in this series of experiments, transmission at the interface is a product of both the contact pressure, as well as the interface coupling as a consequence of the glued layer. Therefore, standard relationships between reflection coefficient, interfacial stiffness and contact pressure are no longer valid, as the relative contributions from asperity interactions and the glued layer with respect to ultrasonic transmission are unknown. Therefore, in these experiments, the reference value has been recorded with the interface assembled (i.e. in contact and glued) prior to the tests starting, and is similarly used to remove attenuation when divided into the measured reflected signal, but now highlights the degree of contact relative to the initial case. In this way, the reflection coefficients presented are 1 at the start of the test, and may rise or fall depending on the loading or unloading and relative level of damage to the glued layer at the interface.

4.1 Lap joints and IBJ sections

Table 2 shows the results of the lap-shear tests. As shown, the load increases approximately at a constant rate from zero to a maximum value when failure occurs. In both cases, rupture occurs rapidly and the shear load subsequently decreases to zero, showing that the adhesive joints only performed elastically under shear load.

Table 2: Results of the tensile lap-shear test of insulated adhesive joints.

Liner type	Dynamic reflection coefficient	Failed joint specimen
Pultruded glass fibre	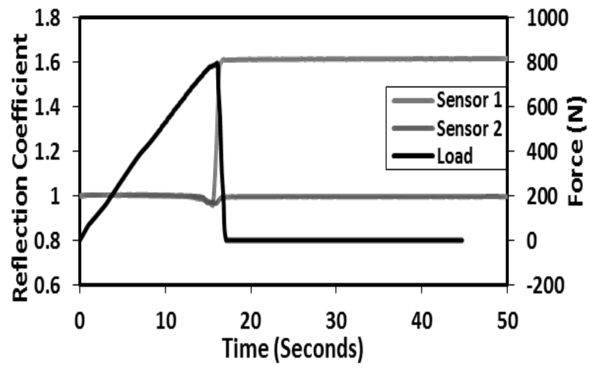	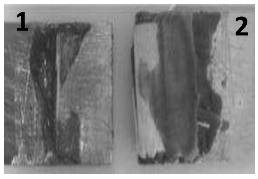
Flexible glass fibre	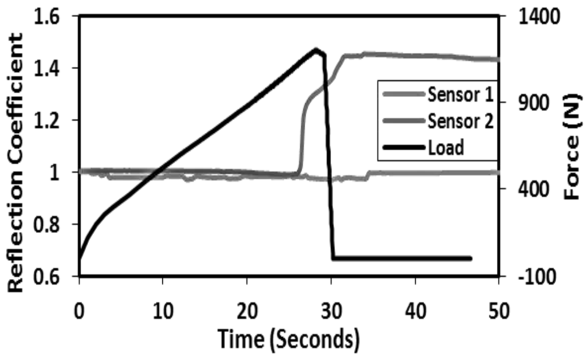	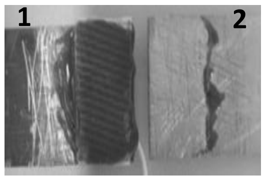

As highlighted by both results, the dynamic reflection coefficient remains at a value of 1, and then rapidly increases on the side of the joint where the glue layer shears. Post-test inspection of the specimens confirmed this observation, with the glued layer still being attached to the side of the specimen maintaining a reflection coefficient of 1, and removed from the side displaying the rapid increase in value.

Overall, failure loads were similar in each case, with associated rises in reflection coefficient also comparable. Based on the fact the same glue was used in each case, this result would be expected. However, the flexible glass fibre specimen appears to have greater endurance. It is also interesting to note that in the case of the pultruded glass fibre test sample, a dip in reflection coefficient occurs prior to the onset of failure. This behaviour suggests an increased lateral load on the joint, and is likely to be associated with twisting of the specimen as failure initiates.

Figure 7 shows the results of the shear tests conducted on the two fishplates, where both the applied load along with the measured reflection coefficients from the previously detailed six sensor locations are shown. Similar failure loads were recorded in each case, where the value of the applied shear load increases from 0 to a maximum when the fishplates are sheared. Additionally, as in the case of the lap joints, elastic behaviour is also observed. It should also be noted that the tests were run under displacement control, accounting for the observed variation in load rate. As shown in both cases, reflection coefficients remain approximately uniform until approximately 90% of the shear load at failure has been applied. At this point, as failure begins to initiate, an increase in reflection coefficient for some of the sensors is observed. Sites where reflection coefficient increases were observed were investigated post-test, and found to correlate with where de-bonding had occurred, with the relative rise in reflection coefficient also linked to the degree of de-bond present. An exception occurs for the flexible glass fibre sheet specimen on the web side, where an early failure was detected. However, this does not appear to prejudice the overall integrity of the specimen, suggesting the failure is localised. Finally, it should also be noted that the flexible glass fibre specimen sustained a small amount of shear load post-failure, and in this case some shearing of the liner material was also observed.

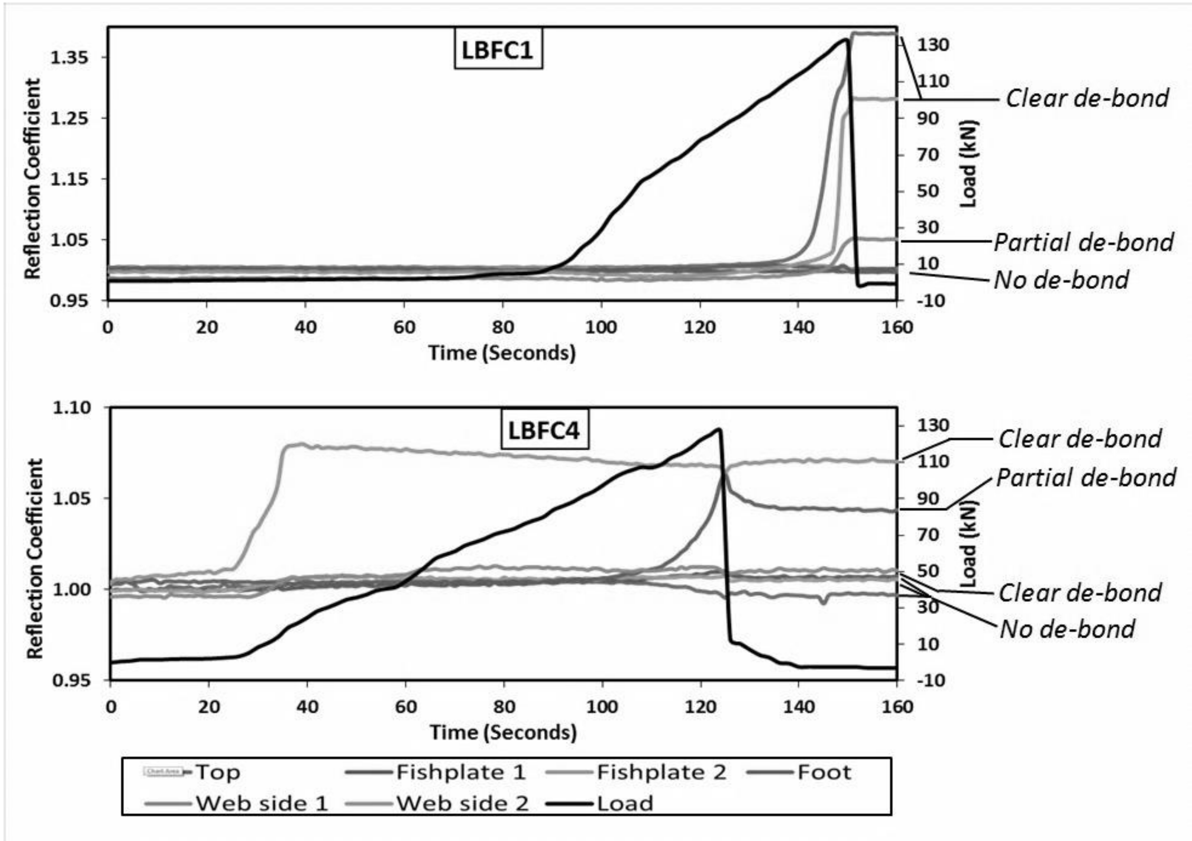

Figure 7: Measured reflection coefficients and shear load during the shearing test of IBJs with pultruded glass fibre (LBFC1) and flexible glass fibre sheet (LBFC4)

4.2 Full IBJs

As shown in Figure 8, fatigue failure occurred in the two IBJs at approximately 1.7 and 1.5 million cycles for the joints with pultruded glass reinforced polyester resin (LBFR1) and glass fibre sheet (LBFR2) respectively. The results of the deflection and the corresponding measured reflection coefficients from the interface of the IBJs during the tests are shown in Figure 9. It should also be noted that Sensor 4 during the first IBJ test (LBFR1) was damaged during set-up, and no measurement was recorded from this sensor.

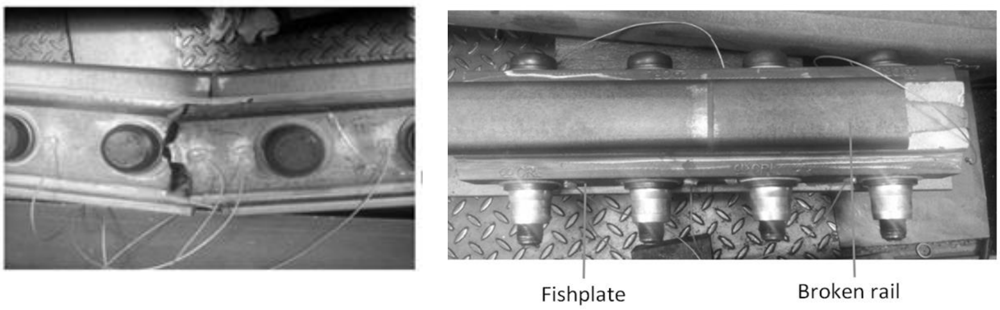

(a) (b)

Figure 8: The failed test specimens (a) LBFR1 IBJ and (b) LBFR2 IBJ.

As shown in Figure 9, for the first three load cycles (161 kN, 270 kN and 337 kN), the displacement of both IBJs remained constant. This indicated that the glue at the interface was intact, and the joint elastic, with a linear relationship between the load and the average deflection at the centre of the joint. For LBFR1 at a load of 404 kN, the deflection at the centre is no longer constant, and started to show plastic behaviour before fatigue of the fishplates (Figure 9 (a)). In contrast, LBFR2 exhibited a linear relation throughout the loading cycles without any sign of plastic behaviour prior to the time of the failure of the rail (Figure 9 (b)). This indicated that the joint to a degree was still intact up to this point

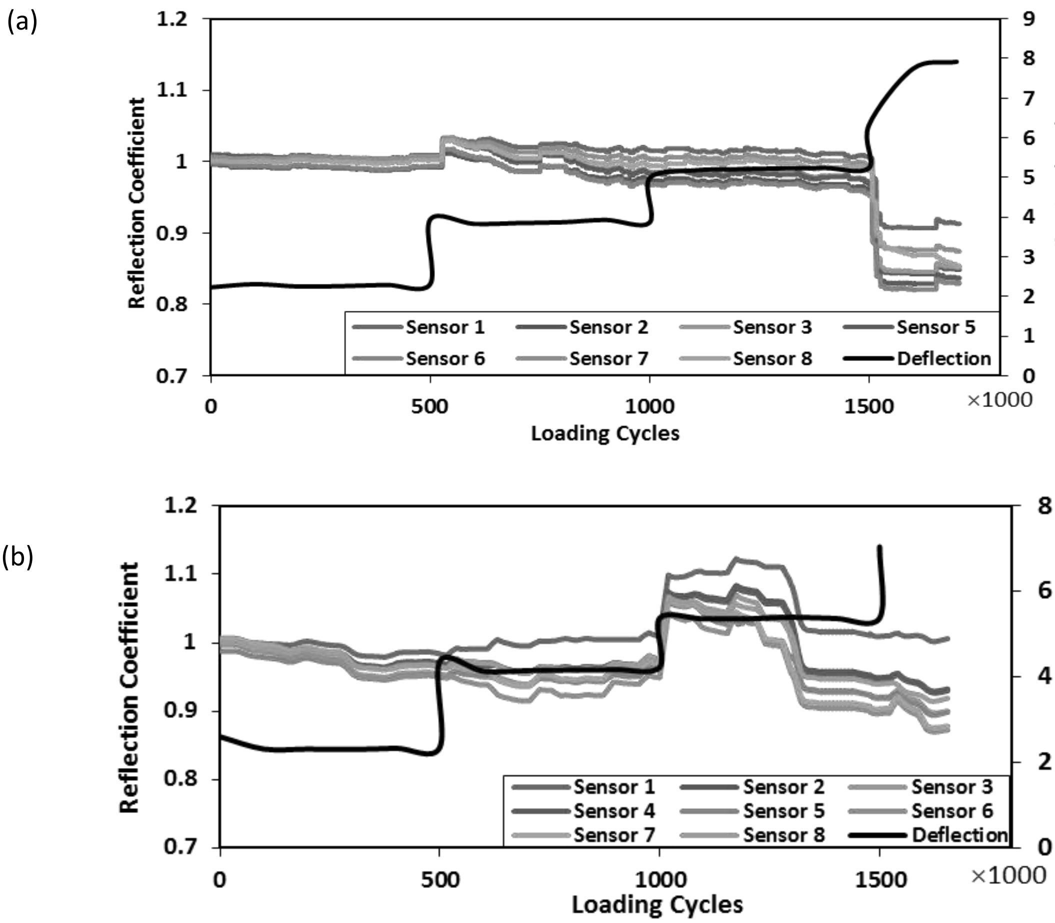

Figure 9: Measured reflection coefficients and deflection at the centre of (a) the LBFR1 IBJ and (b) the LBFR2 IBJ.

In both tests, the measured reflections coefficients initially show similar trends, but with apparent differences as the load cycles increase. In the case of LBFR1, an increase in the value of reflection coefficient was observed at around ½ million cycles (270 kN), indicating separation at the interface and potential failure of the adhesive bond, and was in line with observations made in the lap-joint and shear tests. Over the next 1 million cycles (loads of 270 kN and 337 kN) the reflection coefficient was observed to gradually decrease. Additionally as shown in Figure 10a, wear debris in the form of a powdery substance was also observed at the foot of the rail, further suggesting failure of the glued layer. Finally, upon application of the 404 kN load, the reflection coefficient showed a rapid decrease in the first loading cycles. This behaviour indicated a final failure in the adhesive joint, and the IBJ subsequently failed.

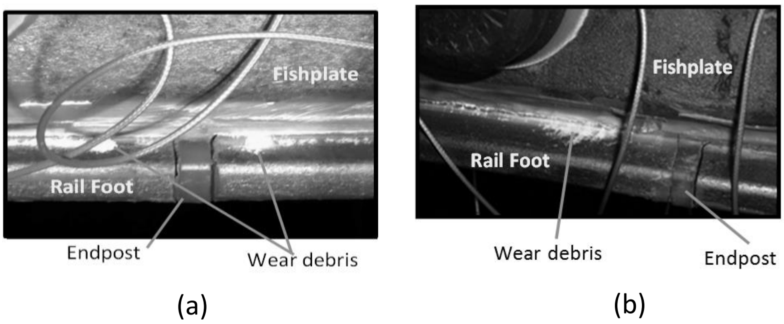

Figure 10: Condition of (a) LBFR1 IBJ after 1½ million loading cycles and (b) LBFR2 IBJ after 1½ million loading cycles

In the case of LBFR2, the reflection coefficients in general show a gradual decrease followed by a sudden increase when the load of 337 kN was applied. Based on the shear test results, this suggests potential twist of the IBJ resulting in an increase in contact at the interface, followed by a sudden failure in the glue layer. It is also interesting to note that this decrease varies in degree between the sensors, with the change more pronounced on one side of the specimen (sensors 5, 6, and 7), further suggesting a torsional effect. Apparent failure of the adhesive layer also occurs later for LBFR2 compared to LBFR1, with this being consistent with both the lap-joint and shear tests, and a consequence of the flexible glass liner being a woven material to which it is easier for the glue to impregnate, giving a better resistance to clean bonding. A similar decrease in reflection coefficient to LBFR1 is also observed post-failure of the bond, with wear debris once again evident (Figure 10b). However, in this case, total failure of the joint did not occur due to simultaneous failure of the rail.

5. DISCUSSION

IBJ's are a combination of adhesive and bolted joints. They are known to be stiffer than conventional conductive rail joints due to the additional contribution of the adhesive bond to the joint. As highlighted in this study, failure of the IBJ starts with deterioration of the adhesive at the interface, and continues until eventual failure of the bond. In all of the different specimens this failure was clearly evident, and corresponded with a rapid increase in the reflection coefficient. However, in the case of the IBJ's, post-failure of the bond, perhaps less intuitive was a decrease in reflection coefficient. Failure of the joints was identified through changes in reflection coefficient of 5% and upwards. As noted the digitiser used was 12-bit, and a voltage range of 5V used on the receiving channel. Typical measured reflected voltages were of the order of 4V, with a measurement error of 1.22mV through digitisation, and when combining errors in the context of a reflection coefficient change of 5%, the absolute error is less than 0.1%. Hence, the measurement error was deemed acceptable to identify joint failures.

The gradual decrease in reflection coefficient observed for the joints as a consequence of failure of the glued layer, can be explained by considering the fastening mechanism that exists in IBJs (Figure 11), and the consequence of slip and fretting wear once the glue de-bonds. As shown in the Figure, wear of the insulating layer leads to greater interface conformity. This behaviour has been previously investigated in conductivity tests on worn IBJs, where once the glue layer has worn, the joint has been found to become similar to a regular conductive rail joint [13]. Such conformity and metal-on-metal contact, will lead to increased transmission of the ultrasonic signal at the interface. Whilst this effect will to a degree be counteracted by a reducing tension in the bolts (as a consequence of reduced extension), leading to a lower load at the interface (and contact pressure) and increased reflection, it appears this is secondary compared to the removal of the acoustic mis-match.

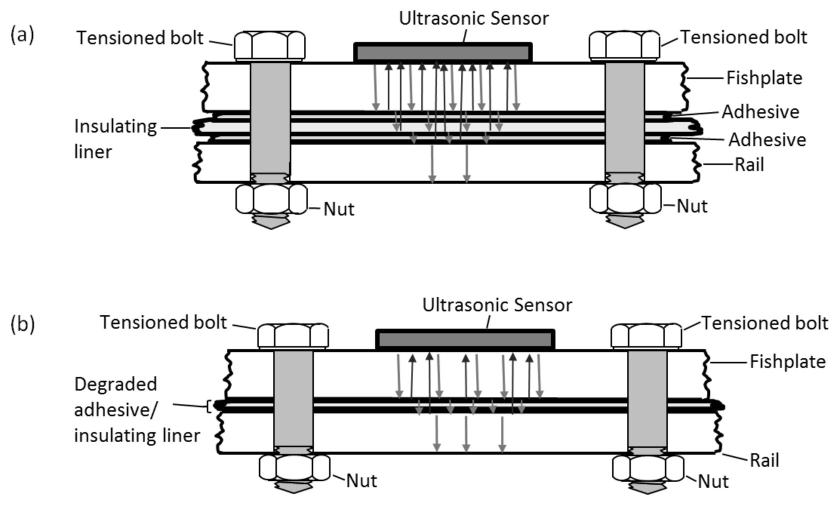

Figure 11: Adhesive insulated bolted joint (a) joint before the degradation of the insulating layer and (b) joint with a degraded insulating layer.

It is also interesting to note, the total failure of the insulating layer (as seen in LBFR1) also led to a sudden decrease in reflection coefficient. This again can be explained in terms of the mechanics of an IBJ. Immediately after the failure of the joint, the majority of the applied load is transferred to the fishplates, as the adhesive bond and bolted fasteners can no longer support it. This causes the measured deflection and observed plastic deformation of the fishplates, leading to an increased interface load and the sudden drop in reflection coefficient.

The four-point loading of the test specimens introduced a uniform stress in the IBJs, and this implies that the interface of the joints will experience equal changes during the test. In the case of LBFR2 this was not the case, and it became apparent that an imbalance has occurred. From the results, whilst the imbalance is obvious in the reflection coefficient data, it is less clear as to whether it is a consequence of the gradual failure of the IBJ, a consequence of its preparation, or indeed the load applicators used in the test apparatus. Whilst it is positive that the technique has the capability to identify inappropriate loading, this result does also highlight a further challenge in its application. In particular, the conclusion with regards to the drop in reflection coefficient being a consequence of twist as opposed to failure of the glued layer was made through knowledge of the applied load. This would not be the case necessarily in a real world application, but could be to a degree resolved by additional monitoring of the bolted joints [18].

Overall, results of this study have shown a promising first step in the use of ultrasound as a condition monitoring tool for IBJs. A next step would be to undertake field trials, where the effect of varying load conditions could be explored. However, prior to this a full-scale test would be carried out in a linear wheel/rail rig in which more typical dynamic loads and movement of the load application point could be achieved that are not present in the current testing set-up. Additionally, as ultrasonic techniques continue to develop, and with many small-scale systems now on the market, the prospect exists for the development of a smart sensor in the long term, which could be used to assess the health of IBJs. This could provide a useful tool for planning preventative maintenance procedures, as it would be capable of directly inferring conditions at the glued interface, a key failure site. However, further work is required to determine and compensate for the effects of environmental conditions, as any moisture ingress to the joints would lead to changes in interface conditions and measured reflection coefficients. Finally, such a tool would also be independent of transient factors such as joint response to dynamic vehicle load, and modulus of the track bed.

6. CONCLUSIONS

A reflection based ultrasonic approach has been used to condition monitor IBJs through to failure, under the application of a dynamic shear load. Specifically, the technique monitored the glued interface, a key failure site in IBJs, using a normally incident longitudinal ultrasound wave. Measured reflection coefficients indicate that the failure of IBJs started with the degradation of the adhesive insulating layer.

Measured reflection coefficients were found to show a sudden increase at the on-set of de-bonding, followed by a gradual decrease as the adhesive layer sustained wear. Upon total failure, load was transferred to the fishplates, and a further abrupt drop in reflection coefficient was observed as a consequence of the now increased interface loading.

The results of this study have shown that ultrasound can be used to monitor the condition of IBJs. The next step is to consider the impact of more representative and transient loads on the ability of the technique to monitor IBJ condition. One approach to this could be to develop a small, smart sensor for monitoring IBJ condition as part of a field trial.

Acknowledgement

The research presented in this paper was undertaken as part of a PhD study by J.T. Stephen at The University of Sheffield, into the condition monitoring of bolted joints in the rail sector, with the final thesis title 'Condition Monitoring of Bolted Joints.'

References

1. Kerr AD and Cox JE. Analysis and tests of boned insulted rail joints subjected to vertical wheel loads. *International Journal of Mechanical Sciences* 1999; 41(10): 1253-1272.
2. Beaty P, Lewis R, Temple B, Marshall MB. Experimental Modelling of Rail End Lipping in Insulated Joints. In: *Proceedings of WCRR*, Sydney, Australia, 2013.
3. Nishihara T. Development of TPC railroad ties for rail joint use. In: *Proceedings of WCRR*, Sydney, Australia, 2013.
4. Zong N and Dhanasekar M. Experimental studies on the performance of rail joints with modified wheel/railhead contact. *Proceedings of the Institution of Mechanical Engineers, Part F: Journal of Rail and Rapid Transit* 2014; 228(8): 857-877.
5. Wen Z, Jin X, and Zhang W, Contact-impact stress analysis of rail joint region using the dynamic finite element method. *Wear* 2005; 258(7): 1301-1309.
6. Chen Y-C and Chen L-W, Effects of insulated rail joint on the wheel/rail contact stresses under the condition of partial slip. *Wear* 2006. 260(11–12): 1267-1273.
7. Ekberg A and Sandström J, Numerical study of the mechanical deterioration of insulated rail joints. *Proceedings of the Institution of Mechanical Engineers, Part F: Journal of Rail and Rapid Transit* 2009; 223(3): 265-273.

8. Mayville RA and Stringfellow RG, Numerical analysis of a railroad bolt hole fracture problem. *Theoretical and Applied Fracture Mechanics* 1995; 24(1): 1-12.

9. Sih GC and Tzou DY, Rail-end bolt hole fatigue crack in three dimensions. *Theoretical and Applied Fracture Mechanics* 1985; 3(2): 97-111.

10. Dhanasekar M and Bayissa W, Performance of square and inclined insulated rail joints based on field strain measurements. *Proceedings of the Institution of Mechanical Engineers, Part F: Journal of Rail and Rapid Transit* 2012; 226(2): 140-154.

11. Health and Safety Investigation Board. *Train Derailment at Potters Bar, UK,* Report, 10 May 2002, SMIS Ref. No.: QNE/2002/02/71643, No. 04655675,2003. p. 1-24.

12. Rail Accident Investigation Branch. *Rail Accident Report – Derailment at Grayrigg 23 February 2007,* Department for Transport, Report no. 081023_R202008_Grayringg_v5, pp. 123-131.

13. Peltier DC and Barkan CPL, Modelling the effects of epoxy debonding on bonded insulated rail joints subjected to longitudianl loads. In: *Transportation Research Board 87th Annual Meeting*. 2008: Washington DC.

14. Davis DD, Akhtar M, Kohake E, and Horizny K. Effects of heavy axle loads on bonded insulated joint performance. In *Proceedings of the AREMA 2005 Annual Conference*. 2005.

15. Davis DD, and Akhtar M, Improving the performance of bonded insulated joints. *Railway track and structures* 2005; 101(1): 14-17

16. Stephen J, Marshall MB, and Lewis R, An investigation into contact pressure distribution in bolted joints. *Proceedings of the Institution of Mechanical Engineers, Part C: Journal of Mechanical Engineering Science* 2014; 228(18): 3405-3418.

17. Marshall M, Lewis R, Drinkwater B, and Dwyer-Joyce RS, An ultrasonic approach for contact stress mapping in machine joints and concentrated contacts. *The Journal of Strain Analysis for Engineering Design* 2004; 39(4): 339-350.

18. Stephen J, Marshall M, and Lewis R, Relaxation of contact pressure and self-loosening in dynamic bolted joints. *Proceedings of the Institution of Mechanical Engineers, Part C:*

Journal of Mechanical Engineering Science. Epub ahead of print 5 May 2016; DOI: 10.1177/0954406216645130.

19. Weight JP, New transducers for high-resolution ultrasonic testing. *NDT International* 1984; 17(1): 3-8.

20. Guyott CCH and Cawley P, Evaluation of the cohesive properties of adhesive joints using ultrasonic spectroscopy. *NDT International* 1988; 21(4): 233-240.

21. Titov SA, Maev RG, and Bogachenkov AN, Pulse-echo NDT of adhesively bonded joints in automotive assemblies. *Ultrasonics* 2008; 48(6-7): 537-546.

22. William JA, *Engineering Tribology*. New York: Cambridge University Press, 2005.

23. Kendall K. and Tabor D, Ultrasonic Study of Area of Contact between Stationary and Sliding Surfaces. *Proceedings of the Royal Society of London Series a-Mathematical and Physical Sciences* 1971; 323(1554): 321-340.

24. Tattersall AG, Ultrasonic Pulse-Echo Technique as Applied to Adhesion Testing. *Journal of Physics D-Applied Physics* 1973; 6(7): 819-832.

25. Drinkwater BW, DwyerJoyce RS, and Cawley P, A study of the interaction between ultrasound and a partially contacting solid-solid interface. *Proceedings of the Royal Society of London Series a-Mathematical Physical and Engineering Sciences* 1996; 452(1955): 2613-2628.

26. Hammant B, The use of 4-point loading tests to determine mechanical properties. *Composites* 1971; 2(4): 246-249.

27. The Permanent Way Institution. *The railway track as a structure.* Report: British Railway Track, Great Britain. 2007. p. 471-486.

28. Standards Austalia, AS1085:12 Railway Track Material Part 12: Insulated Joint Assemblies, Sydney: Standards Australia International Ltd., 2013.